Charge-Transfer Complexes of Tetracyanoethylene with Alkyl, Alkenyl, and Aryl Derivatives of Oxygen

John E. Frey,* Theresa Aiello, Douglas N. Beaman, Scott D. Combs, Shi-lin Fu, and Jeffrey J. Puckett

Department of Chemistry, Northern Michigan University, Marquette, Michigan 49855

Received July 26, 1993®

Spectral characteristics (λ_{CT}, $\Delta\nu_{1/2}$, ϵ) and association constants (K) of charge-transfer (CT) complexes of tetracyanoethylene with donors containing a C–O bond (in CH_2Cl_2 solution) are presented and evaluated. The donors include alcohols, phenols, alkyl, aryl and vinyl ethers, peroxides, furans, anisoles, and polymethoxyarenes. The donor orbitals from which CT transitions originate are determined by the correlation of λ_{CT} and $\Delta\nu_{1/2}$ values of CT bands of the complexes with the ionization bands of the photoelectron spectra of the donor molecules. Relationships between λ_{CT} and K values with respect to the number, geometry, and bulk of substituent groups are established for alkylphenols and -anisoles. Alcohols, alkyl ethers, and cyclic aryloxy compounds donate electrons from the highest occupied nonbonding, n(b_1), orbital of the oxygen atom to the π^* orbital of TCNE to form weak CT complexes which exhibit a single absorbance band. The λ_{max} depends upon the identity of alkyl substituent, increasing in the order of the inductive effect for acyclic alkyls, (Me < Et < *i*-Pr < *t*-Bu) and in the order of ring size (3 < 4 < 5 < 6) for cyclic alkyls. Phenols and aryl ethers donate electrons from the two highest occupied, b_1 and a_2, orbitals to the π^* orbital of TCNE to form CT complexes exhibiting two optical bands. In these donors the oxygen atom bound to the aryl substituent conjugates with phenyl π orbitals through the nonbonded electron pair when the C–O–C moiety is coplanar with the aryl ring. The rotation of phenolic OH groups is not hindered by the presence of *o*-alkyl substituents, whereas the rotation of comparable OMe groups is hindered.

Introduction

Tetracyanoethylene (**T**) is one of the most powerful π-electron acceptors known. Its exceptional reactivity with nucleophiles, including alkenes, arenes, amines, phosphines, alcohols, ketones, thiols, metal alkyls, etc., makes it a valuable and versatile synthetic reagent. Since many of its reactions proceed through the formation of a charge-transfer (CT) complex, often revealed by the appearance of a transitory coloration, it is useful to (1) delimit the scope of the CT interaction, (2) identify the manner in which the interaction is affected by structural,steric, and electronic field effects, (3) determine formation constants and spectral characteristics of CT complexes, and (4) identify the orbitals involved in CT interactions. This paper summarizes the results of a systematic study of the characteristics of the complexes of **T** with molecules which contain single C–O bonds. It presents both formation constants which indicate the degree of thermodynamic potency of the electron donor–acceptor interaction and λ_{CT} values which can be used to identify the donor orbitals involved in the interactions. In particular, we differentiate those molecules in which **T** interacts with oxygen through electrons in localized atomic orbitals from those in which the interaction occurs with electrons in delocalized molecular orbitals.

Merrifield and Phillips[1] first reported the formation of charge-transfer (CT) complexes of tetracyanoethylene (**T**) with alkyl and aryl derivatives of oxygen in dichloromethane (DCM). Since then, numerous investigators, notably Bendig and Kreysig,[2] Pickett et al.,[3] Aliosi et al.,[4] Farrell et al.,[5] Zweig,[6] Voigt and Reid,[7] and Ledwith and Woods[8] have made important contributions to various aspects of the subject.

Our specific objectives are (1) to determine the formation constants (K) and absorbance maxima (λ_{CT}) of CT bands of complexes of **T** with oxygen derivatives, (2) to determine the effects of hydroxy and alkoxy substitution on the orbital energies of benzene rings, (3) to determine the effects of alkyl groups on the energies of the atomic orbitals of oxygen, (4) to determine the specific donor orbitals which give rise to CT interactions by correlating CT bands in the optical spectra of **T** complexes with the ionization bands in photoelectron (PE) spectra, and (5) to integrate our findings with those of previous investigators and to present a comprehensive survey of this area to date.

This report is part of a systematic study of **T** complexes of alkyl and aryl derivatives of elements of Groups 13–17 of the periodic table. Previous papers have covered derivatives of elements in Groups 13[9] and 14 and 15.[10]

T forms transitory CT complexes with many electron-donor molecules. The complex-forming process involves the rapidly reversible transfer of an electron from the HOMO of the donor molecule to the π (b_{3g}) or simply π^* LUMO of the **T** molecule with the simultaneous absorption of a quantum of light, $h\nu$.

® Abstract published in *Advance ACS Abstracts,* March 1, 1994.

[1] Merrifield, R. E.; Phillips, W. D. *J. Am. Chem. Soc.* **1958**, *80*, 2778–2782.

[2] Bendig, J.; Kreysig, D. *Z. Phys. Chem., Leipzig* **1977**, *258*, 1176–1178.

[3] Vars, R.; Tripp, L. A.; Pickett, L. W. *J. Chem. Phys.* **1962**, *66*, 1754–1755.

[4] Aliosi, G. G.; Santini, S.; Savelli, G. *J. Chem. Soc., Faraday Trans. 1* **1975**, *71*, 2045–2050.

[5] Cooper, A. R.; Crowne, C. W. P.; Farrell, P. G. *Trans. Faraday Soc.* **1966**, *62*, 18–28.

[6] Zweig, A. *J. Phys. Chem.* **1963**, *67*, 506–508.

[7] Voigt, E. M. *J. Am. Chem. Soc.* **1964**, *86*, 3611–3617. Voigt, E. M.; Reid, C. *J. Am. Chem. Soc.* **1964**, *86*, 3930–3934.

[8] Ledwith, A.; Woods, H. J. *J. Chem. Soc. B* **1970**, 310–314.

[9] Frey, J. E.; Kitchen, E. C. *J. Am. Chem. Soc.* **1983**, *105*, 2175–2178.

[10] Frey, J. E.; Cole, R. D.; Kitchen, E. C.; Surprenant, L. M.; Sylwestrzak, M. S. *J. Am. Chem. Soc.* **1985**, *107*, 748–755.

0022-3263/94/1959-1817$04.50/0

$$\mathbf{D} + \mathbf{T} \rightleftarrows \mathbf{D}\text{–}\mathbf{T} \overset{h\nu}{\rightleftarrows} \mathbf{D}^+\mathbf{T}^-$$

The frequency of the light absorbed is linearly related to the ionization energy of the electron in the donor molecule. Analysis of the absorbance spectrum of the complex yields spectral properties of the complex as well as its association constant and the CT energy. Correlation of the CT spectrum of the complex with the ionization bands of the photoelectron spectrum of the donor molecule using the empirical equation[11]

$$\lambda_{\mathrm{CT}}\ (\mathrm{nm}) = 1240/(0.81 I_{\mathrm{D}} - 4.28) \quad (1)$$

facilitates the determination of the energy of the donor electrons. Here, λ_{CT} corresponds to $\lambda_{\max}$ for a specific absorbance band of the complex, and I_{D} is the vertical ionization energy of the donor orbital. Equation 1 tends to underestimate the first two CT bands, λ_1 and λ_2, for organooxy compounds by 10–40 and 0–20 nm. The parameters are derived from the analysis of 265 data points; eq 1 has a reliability of ±5% relative.

Experimental Section

Experimental procedures, data collection and processing, and judgmental criteria are described in a previous paper.[12] Most of the spectra in this study were recorded with a Shimadzu UV3101PC UV–vis–NIR spectrophotometer.

Results and Discussion

The results of our and other published studies of **T** complexes of the following types of oxygen containing donors are summarized in Table 1 and the enumerated sections of the text: 1, alcohols (ROH); 2, phenols (ArOH); 3, alkyl ethers (ROR) and peroxides (ROOR); 4, alkyl vinyl ethers (ROCH=CH$_2$); 5, aryl ethers (ArOAr); 6, furans; 7, alkyl phenyl ethers (ROPh); 8, alkyl aryl ethers (ROAr); and 9, polymethoxyarenes. Donors are coded for reference in the text according to the alphanumeric characters shown in column 1 of Table 1.

Complexes of **T** with oxygen donors exhibit one or two CT bands. If one composite band appears in the spectrum it is designated $\lambda_{\max}$ and is inserted in column 3. If one or two simple bands appear in the spectrum they are designated λ_1 and λ_2 and inserted in columns 4 and 5. If a band appears as a shoulder on the solute cutoff, the wavelength at one-half band height is given with an sh suffix. If the main band is deconvoluted into two overlapping bands, λ_1 and λ_2, as well as A_2/A_1 and $\Delta\nu_{1/2}$, are italicized. Molar absorbance values, ϵ, for the band with the largest absorbance value are given in column 6. The ratios of absorbances of λ_2 to λ_1, A_2/A_1, are given in column 7, and the band height at half-width, $\Delta\nu_{1/2}$, is given in column 8. The apparent association constant, K (L/mol), for the complex is reported in column 9. The product ϵK is a measure of the "effective absorbance" of a complex since the larger the value of ϵ and/or K the greater the net absorbance of the complex for a given level of reagent concentrations. The ϵK values, given in column 10, are of interest because their magnitudes are characteristic of the various classes of complexes; in some cases trends in ϵK values follow progressive structural modifications in substituent groups. The ratios of the concentrations of stock solutions of the donor, C_{D}, and of **T**, C_{T}, are given in column 11. The saturation fraction, s, of a complex, that is the molar concentration of the complex divided by the concentration of the limiting reactant, is calculated using the equation $s = A/\epsilon C_{\mathrm{Y}}$ where C_{Y} is the analytical concentration of the limiting reagent. Percent saturation values are given in column 12. Notations in Table 1 which describe the Scott graphs used to calculate ϵ and K are as follows: cur = curved line; neg = negative slope; err = erratic data.

1. Alcohols. Analyses of PE spectra of alcohols indicate that the HOMO's are the nonbonding $2a_2''$ orbitals which are localized on the oxygen; these orbitals are most likely involved in the formation of CT complexes with **T**. For the homologous series of alcohols[13,14] (MeOH, EtOH, *i*-PrOH, and *t*-BuOH), the I_1 values (10.94, 10.64, 10.36, and 10.25 eV) decrease as the number of Me groups bound to the α-carbon atom increases. Substitution of these values into eq 1 yields corresponding λ_1 271, 286, 302, and 308 nm. These values suggest that systems containing tertiary alcohols might yield characterizable CT complexes. Accordingly, we studied a series of systems containing **T** and *tert*-butyl alcohol and 1-adamantol, as well as ethanol and isobutyl alcohol. These alcohol/T/DCM systems exhibit weak bands as shoulders on the **T** cutoff with half-height absorbancies at 330–340 nm which are attributable to $\pi^* \leftarrow \mathrm{n}(a_2'')$ transitions. Analyses of these bands yield Scott lines with strong curvature and poor correlation coefficients indicating that weak 1:1 and possibly 2:1 complexes form in solution. The strong absorbance cutoff of **T** at 310 nm precludes a detailed analysis of these bands.

2. Phenols. Bendig and Kreisig[2] reported λ_{CT} values for systems containing **T** with phenol and several of its alkyl and halo derivatives in DCM. In all cases they found two absorbance bands, λ_1 and λ_2. When the OH group is coplanar with the phenyl ring, the $\mathrm{n}(b_1)$ orbital of the oxygen conjugates with the b_1 orbital of the phenyl ring. This gives rise to a b_1 orbital with a higher energy than that of the corresponding e_{1g} orbital of benzene. Since the point of attachment of the OH group coincides with the node of the a_2 orbital the energy of this orbital is unaffected by conjugation. Consequently, **P–T** exhibits two CT bands which arise from $\pi^* \leftarrow b_1$ and $\lambda^* \leftarrow a_2$ transitions.

a. Phenol. The two maxima in the spectrum of **P–T**, λ_1 483 and λ_2 388 nm (Figure 1), correspond to PE bands at 8.67 and 9.36 eV[15] in **P** which are due to ionizations from the b_1 and a_2 orbitals of the phenyl ring; these I_{D} values yield calculated λ_{CT} of 467 and 383 nm. The good agreement between experimental and calculated values indicates that optimal $\mathrm{n}(b_1)$–$\pi(b_1)$ conjugation occurs in both the solution and vapor phases. Analysis of the optical data yields ϵ and K values of 1370 L/mol-cm and 0.37

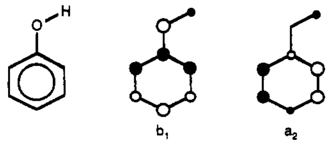

π Molecular Orbitals of Phenol

---

[11] Frey, J. E. *Appl. Spectrosc. Rev.* **1987**, *23*, 247–283.

[12] Frey, J. E.; Andrews, A, M,; Ankoviac, D. G.; Beaman, D. N.; Du Pont, L. E.; Elsner, T. E.; Lang. S. R.; Zwart, M. O.; Seagle, R. E.; Torreano, L. A. *J. Org. Chem.* **1990**, *55*, 606–624.

[13] Katsumata, S,; Iwai, T.; Kimura, K. *Bull. Chem. Soc. Jpn.* **1973**, *46*, 3391–3395.

[14] Robin, M. B.; Kuebler, N. A. *J. Electron Spectrosc.* **1972/73**, *1*, 13–28.

[15] Debies, T. P.; Rabalais, J. W. *J. Electron Spectrosc.* **1972/73**, *1*, 355–370.

Table 1. Complexes of Tetracynaoethylene with Alkyl-, Alkenyl- and Aryloxygen Compounds in Dichloromethane at 22 °C

code	donor compd	λ_{max}	λ_1, nm	λ_2, nm	ϵ_1, L/mol-cm	A_1/A_2	$\Delta\nu_{1/2}$, cm^{-1}	K, L/mol	ϵK	C_D/C_T	% satn
	ethanol		<300 sh							26	
	2-methyl-1-propanol		340 sh		cur					200	
	2-methyl-2-propanol		330 sh		err					100	
	1-adamantol		330 sh							15	
P	phenol		483	388	1370 ± 70	0.83		0.37 ± 0.02	510	91	8–16
	phenol[a]		485	390		0.80					
	phenol[b]		488	381							
	phenol[c]		488	381							
2MP	2-methylphenol		*515*	415	1640 ± 100	0.86		0.63 ± 0.04	1030	20	6–12
	2-methylphenol[b]		512	395							
	2-methylphenol[c]		511	419							
2EP	2-ethylphenol		*514*	*425*	1690 ± 330	0.84		0.52 ± 0.10	880	10	4–8
	2-ethylphenol[c]		517	416							
2IP	2-isopropylphenol		*520*	*430*	2260 ± 760	0.85		0.23 ± 0.08	520	25	3–6
	2-isopropylphenol[c]		522	426							
2SBP	2-*sec*-butylphenol[c]		520	429							
2BP	2-*tert*-butylphenol		*526*	*428*	4320 ± 1810	0.88		0.08 ± 0.03	350	20	1–3
	2-*tert*-butylphenol[c]		524	424							
3MP	3-methylphenol		*510*	*420*	1730 ± 90	0.90		0.61 ± 0.03	1060	99	11–20
	3-methylphenol[b]		497	420							
	3-methylphenol[c]		504	427							
3EP	3-ethylphenol[c]		505	433							
3BP	3-*tert*-butylphenol		*505*	*420*	750 ± 270	*0.70*		0.62 ± 0.22	750	1	2–5
4MP	4-methylphenol		535	394	cur	0.68				1–95	
	4-methylphenol[b]		540	392							
	4-methylphenol[c]		535	401							
4EP	4-ethylphenol		537	394	1440 ± 200	0.68	5700	0.56 ± 0.08	810	25	5–11
	4-ethylphenol[c]		535	394							
4IP	4-isopropylphenol		536	396	980 ± 90	0.68	6600	0.63 ± 0.06	620	25	9–18
4BP	4-*tert*-butylphenol		532	400	cur	0.70	6500			25	
	4-*tert*-butylphenol[c]		529	400							
4OP	4-(1,1,3,3-tetramethyl-*n*-butyl)phenol[c]		538	401							
23MP	2,3-dimethylphenol	500	*540*	*450*	2900 ± 280		7800	0.90 ± 0.09	2610	1/9	3–6
	2,3-dimethylphenol[c]		513 sh	463							
24MP	2,4-dimethylphenol		557	428	2120 ± 70	0.68	5900	1.19 ± 0.04	2520	95	14–28
	2,4-dimethylphenol[c]		562	427							
2B4MP	2-*tert*-butyl-4-methylphenol[c]		533	424							
24BP	2,4-di-*tert*-butylphenol		585	443	440 ± 100	0.95		0.25 ± 0.06	110	9	3–6
	2,4-di-*tert*-butylphenol[c]		577	426							
25MP	2,5-dimethylphenol		*540*	*440*	2610 ± 170	*0.86*		0.91 ± 0.06	2380	96	11–22
	2,5-dimethylphenol[b]		546	450							
2I5MP	2-isopropyl-5-methylphenol[c]		549	463							
5I2MP	5-isopropyl-2-methylphenol[c]		543	465							
26MP	2,6-dimethylphenol	516	*540*	*450*	2840 ± 70	*0.98*	8200	0.90 ± 0.02	2780	93	11–22
	2,6-dimethylphenol[c]		514	465							
2B6MP	2-*tert*-butyl-6-methylphenol		536	470	1380 ± 80	1.00		0.54 ± 0.03	750	23	7–15
26BP	2,6-di-*tert*-butylphenol		564	477	neq	0.92				20	
	2,6-di-*tert*-butylphenol[c]	557									
34MP	3,4-dimethylphenol		558	427	2460 ± 130	0.74	5900	0.91 ± 0.05	2240	49	11–22
	3,4-dimethylphenol		557	422							
35MP	3,5-dimethylphenol	480	*535*	*450*	2830 ± 140		7800	0.75 ± 0.04	2120	94	9–19
	3,5-dimethylphenol[c]	480									
35MP	3,5-di-*tert*-butylphenol	518			neq		7600			22	
235MP	2,3,5-trimethylphenol	515	*565*	*480*	3160 ± 170		7100	1.96 ± 0.11	6190	88	14–27
	2,3,5-trimethylphenol[c]	520									
236MP	2,3,6-trimethylphenol	515	*570*	*480*	3420 ± 100		7000	2.22 ± 0.07	7590	89	15–28
	2,3,6-trimethylphenol[c]	503									
246MP	2,4,6-trimethylphenol		583	467	3370 ± 280	0.78		1.78 ± 0.15	6000	97	12–25
26B4MP	2,6-di-*tert*-butyl-4-methylphenol[c]		630	476							
246BP	2,4,6-tri-*tert*-butylphenol*	530 sh			err					1/10	
345MP	3,4,5-trimethylphenol		574	465	2350 ± 50	0.85		2.29 ± 0.05	5380	93	15–29
2HOP	1,2-dihydroxybenzene		540	430	1420 ± 20	0.74		0.67 ± 0.06	950	22	6–13
	1,2-dihydroxybenzene[c]		542	426							
3HOP	1,3-dihydroxybenzene	505	*535*	*435*	690 ± 40		9100	1.29 ± 0.20	890	1/10	4–9
	1,3-dihydroxybenzene[c]		514	426							
4HOP	1,4-dihydroxybenzene				insol						
	1,4-dihydroxybenzene[a]		580	375		0.67					
	1,4-dihydroxybenzene[c] (in MeCN)		588	381		0.67					
3MOP	3-methoxyphenol[c]		529	455 sh							
4MOP	4-methoxyphenol[c]		610	378							
26MOP	2,6-dimethoxyphenol[c]		575								
35MOP	3,5-dimethoxyphenol[c]		538								
2M3HOP	2-methyl-1,3-dihydroxybenzene	507			2560 ± 290		6500	1.08 ± 0.13	2770	1/10	3–7
	2-methyl-1,3-dihydroxybenzene[c]	512									
2M4HOP	2-methyl-1,4-dihydroxybenzene[c]		623	407							
23HOP	1,2,3-trihydroxybenzene	516			4410 ± 2690		6500	0.46 ± 0.26	2030	1/8	1–3
	1,2,3-trihydroxybenzene[c]	514									
35HOP	1,3,5-trihydroxybenzene[c] (in MeCN)	514									
EEO	ethyl ether		347		neq			<0.01		20	
	ethyl ether[d] (in $CHCl_3$)		335		1100			0.10	110		
IIO	isopropyl ether		348		neq			<0.01		100	

Table 1. (Continued)

code	donor compd	λ_{max}	λ_1, nm	λ_2, nm	ϵ_1, L/mol-cm	A_1/A_2	$\Delta\nu_{1/2}$, cm^{-1}	K, L/mol	ϵK	C_D/C_T	% satn
BMO	*tert*-butyl methyl ether		355				6500	<0.01		100	
BEO	*tert*-butyl ethyl ether		360		cur					20	
BBOO	*tert*-butyl peroxide		385		170 ± 69		9000	0.07 ± 0.03	12	20	2–4
12BO	1,2-butenoxide		315 sh		736 ± 68			1.25 ± 0.13	920	100	21–39
CHO	cyclohexenoxide		318 sh		1190 ± 50			0.88 ± 0.04	1050	25	9–19
	cyclohexenoxide		318 sh		1750 ± 100			0.59 ± 0.04	1030	400	19–34
OXT	oxetane		346		1020 ± 90		5400	0.85 ± 0.07	870	10	7–14
THF	tetrahydrofuran		343		2020 ± 200		6100	0.23 ± 0.02	460	92	6–14
	tetrahydrofuran		340		2040 ± 80		6100	0.21 ± 0.01	430	730	15–29
	tetrahydrofuran^{e} (in $CHCl_3$)		318		3130			0.06	230		
THP	tetrahydropyran		359		857 ± 45		5800	0.54 ± 0.03	460	24	8–16
	tetrahydropyran		357		913 ± 21		5800	0.55 ± 0.01	500	100	15–30
	tetrahydropyran^{e} (in $CHCl_3$)		318		2740			0.05	140		
DOX	dioxane^{e} (in $CHCl_3$)		350		1860			0.12	220		
MVO	methyl vinyl ether^{*,f}		401								
EVO	ethyl vinyl ether^{*,f}		419								
23DHF	2,3-dihydrofuran*		503		740 ± 50		6400	0.29 ± 0.02	220	10	4–10
25DHF	2,5-dihydrofuran*		389		550 ± 70		6500	0.41 ± 0.05	230	9	6–12
34DHP	3,4-dihydro-2*H*-pyran*		487		820 ± 120		6700	0.23 ± 0.03	190	0	3–7
	3,4-dihydro-2*H*-pyran^{*,f}		460								
IVO	2-propyl vinyl ether^{*,f}		430								
	1-butyl vinyl ether*		437				6700				
	2-butyl vinyl ether*		437				6500				
	2-butyl vinyl ether^{*,f}		427								
	cyclohexyl vinyl ether^{*,f}		433								
BVO	*tert*-butyl vinyl ether^{*,f}		436								
MIO	methyl 2-propenyl ether^{*,f}		452								
F	furan		449		780 ± 80		5500	0.32 ± 0.03	250	11	3–6
	furan^{g}		448	310 sh							
	furan^{g} (in CCl_4)							0.56			
	furan^{h} (in $CHCl_3$)		450		1100			0.29 ± 0.02	320		
2MF	2-methylfuran		512	312 sh	1300 ± 80		5300	0.44 ± 0.03	570	23	6–12
3MF	3-methylfuran^{g}		490								
2BF	2-*tert*-butylfuran^{g}		530	330 sh							
3BF	3-*tert*-butylfuran^{g}		490	340 sh							
25MF	2,5-dimethylfuran		574	329	2170 ± 70		5200	0.74 ± 0.03	1610	22	9–18
BF	benzofuran	460	*500*	*425*	2040 ± 90		8000	0.32 ± 0.01	650	20	3–7
	benzofuran^{h} (in $CHCl_3$)	465			1100			1.07 ± 0.04	1180		
DBF	dibenzofuran	500	*525*	*485*	603 ± 51		6200	1.36 ± 0.12	820	1/10	5–10
	dibenzofuran^{h} (in $CHCl_3$)	498			1650			1.05 ± 0.04	1730		
PPO	phenyl ether		495	377	810 ± 50	1.55	6800	0.39 ± 0.01	320	10	5–10
XAN	xanthene		575	375	370 ± 30	0.83	5100	2.35 ± 0.18	870	1/10	9–19
A	anisole		511	389	1360 ± 80	0.80		0.47 ± 0.03	640	25	5–12
	anisole^{d}		507	384	2080	0.79		0.28	580		
	anisole^{f}		509	387							
	anisole^{j}		508	383							
	anisole^{a}		507	387		0.78					
	anisole^{f}		505	385	2220	0.84		0.27	600		
	anisole^{b}		485	385							
	anisole^{k}		508	391							
	anisole^{l}		508								
	anisole^{c}		508	383							
EPO	phenetole		521	391	1330 ± 80	0.77		0.52 ± 0.03	690	31	6–13
	phenetole^{j}		518	385							
	phenetole^{f}		513	387	1540			0.48	740		
IPO	isopropoxybenzene^{f}		522	391	2000			0.26	520		
2MBPO	2-methylbutoxybenzene^{f}		521	390	1670			0.4	670		
BPO	*tert*-butoxybenzene^{f}		*462*	*390*	1300			0.43	560		
APO	allyl phenyl ether^{l}		512								
VPO	vinyl phenyl ether^{l}		484								
2MA	2-methylanisole		547	422	970 ± 80	0.82		1.51 ± 0.13	1470	9	8–17
	2-methylanisole^{j}		546	420		0.8					
			546	*418*		*0.8*	*4700, 5400*				
	2,3-dihydrobenzofuran		567	405	980 ± 80	0.66	5100, 5700	1.08 ± 0.08	1060	10	6–12
3MA	3-methylanisole		532	425	cur	0.87				8	
	3-methylanisole^{j}		532	427							
			532	*417*		0.8	4600, 5500				
4MA	4-methylanisole		563	396	1350 ± 130	0.70	5600, 5200	0.98 ± 0.10	1320	25	9–18
	4-methylanisole^{a}		563	395		0.60					
	4-methylanisole^{j}		562	395		0.7	4800, 5600				
23MA	2,3-dimethylanisole	550	*560*	*465*	1970 ± 150	1.01		1.47 ± 0.12	2900	21	8–17
24MA	2,4-dimethylanisole		594	431	3200 ± 610	0.69		0.87 ± 0.16	2780	7	3–7
	2,4-dimethylanisole		592	431	3260 ± 550	0.70		0.91 ± 0.15	2970	26	5–11
25MA	2,5-dimethylanisole		547	454	2410 ± 320	0.71		1.37 ± 0.18	2410	23	8–16
26MA	2,6-dimethylanisole	458	*475*	*445*	2500 ± 100		6200	0.55 ± 0.02	1380	27	4–10
34MA	3,4-dimethylanisole		586	429	2160 ± 160	0.75		1.26 ± 0.09	2590	25	7–14
35MA	3,5-dimethylanisole	539	*545*	*465*	1200 ± 70	0.99		2.26 ± 0.13	2710	24	13–25
2PA	2-phenylanisole		550	415	880 ± 100	1.01		0.77 ± 0.08	680	10	6–12
	2-phenylanisole^{j}		*549*	*413*		*1.0*	*4800, 6000*				
4PA	4-phenylanisole		600	375	1010 ± 120	1.03	5300, 7000	0.83 ± 0.10	840	10	6–12
	4-phenylanisole^{j}		*602*	*373*		*1.8*	*5300, 6700*				

Table 1. (Continued)

code	donor compd	λ_{max}	λ_1, nm	λ_2, nm	ϵ_1, L/mol-cm	A_1/A_2	$\Delta\nu_{1/2}$, cm^{-1}	*K*, L/mol	ϵK	C_D/C_T	% satn
2MOA	1,2-dimethoxybenzene		593	436	1320 ± 40	0.54		1.12 ± 0.04	1480	20	12–23
	1,2-dimethoxybenzene[f]		592	433							
	1,2-dimethoxybenzene[j]		592	429							
BDL	1,3-benzodioxole		578	400	1270 ± 120	0.74	5500, 6400	0.35 ± 0.03	430	8	3–7
	1,3-benzodioxole[m]		575								
BDN	1,4-benzodioxan		556	444	1860 ± 250	0.90		0.27 ± 0.04	500	10	3–7
3MOA	1,3-dimethoxybenzene	546	*550*	*480 sh*	1830 ± 90			0.68 ± 0.03	1240	11	4–9
	1,3-dimethoxybenzene[i]		548	470 sh							
	1,3-dimethoxybenzene[j]		*559*	*441*							
4MOA	1,4-dimethoxybenzene		634	382	1770 ± 80	0.56	5800, 5400	0.68 ± 0.03	1200	18	8–16
	1,4-dimethoxybenzene[i]		621	380							
	1,4-dimethoxybenzene[a]		621	380		0.50					
	1,4-dimethoxybenzene[j]		637	380							
23MOA	1,2,3-trimethoxybenzene	515			1520 ± 50		6400	2.24 ± 0.10	2690	11	10–21
	1,2,3-trimethoxybenzene[i]	515									
	1,2,3-trimethoxybenzene[j]	515									
	1-methoxy-2,3-(methylenedioxy)benzene[a]	530									
24MOA	1,2,4-trimethoxybenzene		690	449	1860 ± 100	0.34	5900	1.75 ± 0.09	3260	19	10–21
	1,2,4-trimethoxybenzene[f]		686	447							
	1,2,4-trimethoxybenzene[j]		685	427							
35MOA	1,3,5-trimethoxybenzene		551	318	1900 ± 210	0.39	5800	1.80 ± 0.20	3420	1/9	6–12
	1,3,5-trimethoxybenzene[f]		552								
234MOA	1,2,3,4-tetramethoxybenzene[f]		560	480							
235MOA	1,2,3,5-tetramethoxybenzene	606			1350 ± 140		6900	3.79 ± 0.41	5120	1/10	10–21
	1,2,3,5-tetramethoxybenzene[f]	605									
245MOA	1,2,4,5-tetramethoxybenzene[f]		800	440							
PMOB	pentamethoxybenzene[f]	610									
HMOB	hexamethoxybenzene[f]		512								

* Reacts with TCNE. [a] Zweig, A. *Tetrahedron Lett.* 1964, 89–94. [b] Reference 2. [c] Reference 19. [d] Reference 1. [e] Reference 3. [f] Reference 8. [g] Reference 4. [h] Reference 5. [i] Reference 6. [j] Reference 7. [k] Timpe, H.-J.; Weschke, W. *Z. Prakt. Chem.* 1981, *323*, 345–348. [l] Chmutova, G. A.; Podkovyrina, T. A. *J. Gen. Chem. USSR (Engl. Transl.)* 1975, *45*, 145–149; *Zh. Obshch. Khim.* 1975, *45*, 158–164. [m] Reference 45.

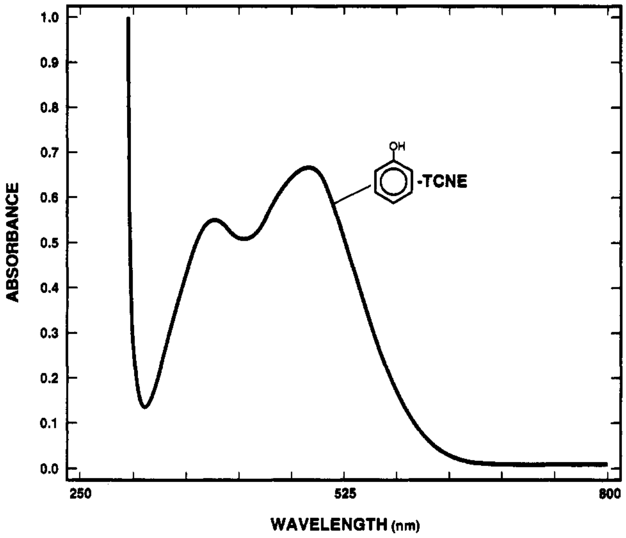

Figure 1. Spectrum of phenol–T.

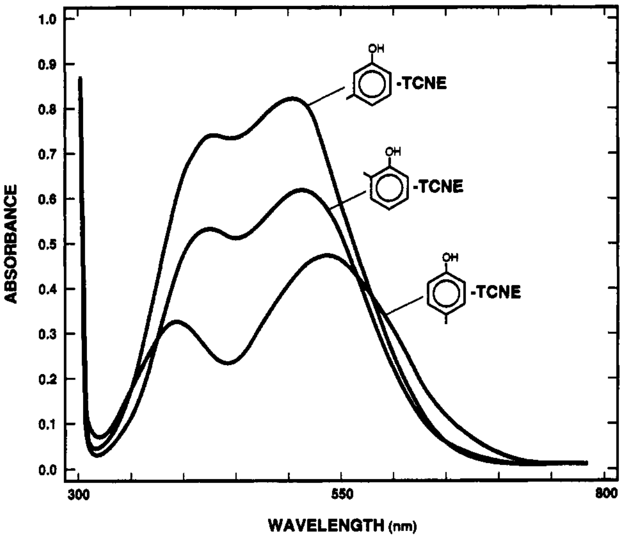

Figure 2. Spectra of 2-, 3-, and 4-methylphenol–T.

L/mol. A slight curvature in the Scott line suggests the presence of 2:1 complexes.

b. Monoalkylphenols. This section includes complexes of T with the methyl, ethyl, isopropyl, and *tert*-butyl phenols.

i. 2-Alkylphenols. The spectrum of **2MP–T** (Figure 2) consists of overlapping bands at λ_1 *515* nm and λ_2 *415*; these wavelengths correspond to PE ionizations at 8.48 and 9.08 eV[15] which lead to calculated values of 479 and 403 nm. The wavelength shifts of **2MP–T** relative to **P–T**, $\Delta\lambda_1$ 29 and $\Delta\lambda_2$ 33 nm, are attributed to the inductive effect of the methyl on both the and b_1 and a_2 orbitals of the phenol group. The corresponding λ_1 and λ_2 values for **2EP–T**, **2IP–T**, and **2BP–T** range from 514–526 to 425–430 nm. The fact that both shifts tend to increase in the order Me < Et < *i*-Pr < *t*-Bu indicates that the inductive effects of these groups on the b_1 and a_2 orbitals increase in the same order. However, the *K* values at 0.63, 0.52, 0.23, and 0.08 L/mol decrease progressively with the bulk of the alkyl group as the intermolecular contact between the donor and T molecules becomes increasingly hindered.

ii. 3-Alkylphenols. The spectrum of **3MP–T** has CT bands at *510* and 420 nm which correspond to wavelength shifts $\Delta\lambda_1$ *31* and $\Delta\lambda_2$ 27 nm. These shifts are attributed to the inductive effects of the 3-methyl group on both the b_1 and a_2 orbitals of the phenyl ring. The PE spectrum of **3MP** exhibits ionization bands at 8.48 and 9.08 eV[16] which lead to calculated values of λ_1 479 and λ_2 403 nm. The *K* values of **2MP–T** and **3MP–T** at 0.63 and 0.61 L/mol are nearly identical as expected from their structural similarity.

---

(16) Kobayashi, T.; Nagakura, S. *Bull. Chem. Soc. Jpn.* **1974**, *47*, 2563–2572.

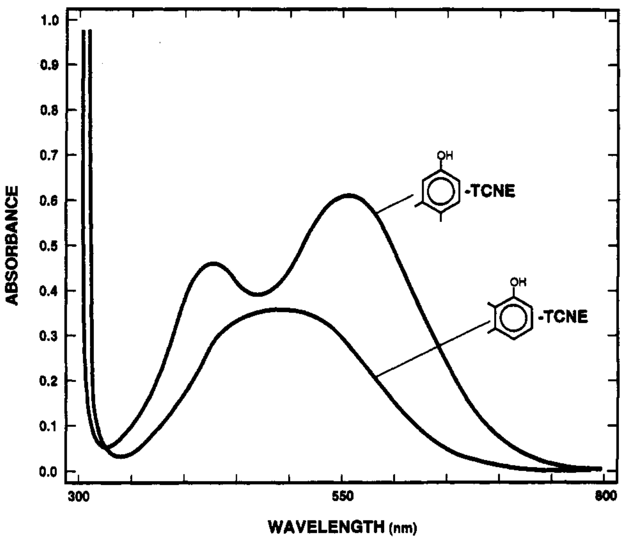

Figure 3. Spectra of 2,3- and 3,4-dimethylphenol–T.

iii. 4-Alkylphenols. The spectrum of **4MP–T** has bands at λ_1 535 and λ_2 394 nm. The λ_2 band is nearly identical with that of corresponding band for **P–T** indicating that the a_2 orbital is unaffected by the 4-Me group. The large difference between λ_1 and λ_2 values (140 nm) is attributed to the ability of the 4-Me group to inductively supplement the strong conjugative effect of the OH group on the b_1 orbital without affecting the a_2 orbital. The PE ionizations of **4MP** at 8.38 and 9.25 eV[16] lead to calculated λ_{CT} values of 494 and 386 nm for **4MP–T**. The strong curvature of the Scott line for this complex suggests the presence of appreciable amounts of the 2:1 complex in the system.

The λ_1 and λ_2 values of **4MP–T**, **4EP–T**, **4IP–T**, and **4BP–T** are practically identical, showing only a negligible alkyl substituent effect in this series. Data for the 3- and 4-alkylphenol–T complexes are not sufficient to discern trends in *K*.

c. Dialkylphenols. All six possible dimethylphenol–T complexes are characterized. Values of ϵ and *K* for all 1:1 complexes fall into narrow ranges of 2100–2900 L/mol-cm and 0.75–1.20 L/mol. It is convenient to divide the donors into two groups: (i) those which contain a 4-Me group and (ii) those which do not.

i. 24MP–T and 34MP–T. The spectra of these complexes (Figure 3) are nearly identical, each having λ_1 557–558 and λ_2 427–428 nm with a deep minimum between the peaks. The PE ionizations of **24MP** at 8.18 and 8.89 eV[16] yield calculated values of 529 and 425 nm.

ii. 23MP–T, 25MP–T, 26MP–T, and 35MP–T. The λ_1 and λ_2 bands for these complexes overlap so strongly that none of them shows a minimum between the peaks. The λ_1 (*540* nm) and λ_2 (*440–450* nm) values for **25MP–T** and **26MP–T** are estimated by deconvolution of the optical spectra. Both λ_1 and λ_2 increase by 52–62 nm relative to the corresponding **P-T** bands due to the additive inductive effect of the two methyls on the b_1 and a_2 orbitals.

The fact that λ_{max} for **26MP–T** (516 nm) is not lower than that for **35MP–T** (480 nm) indicates that the *o*-Me's on **26MP** do not hinder the rotation of the OH group sufficiently to inhibit n(p)–π(b_1) conjugation. Maier and Turner[17] reached the same conclusion on the basis of their PE study of **26MP**. Of greater interest is the fact that both λ_1 and λ_2 tend to increase for the series of complexes **26MP–T**, **2B6MP–T**, and **26BP–T**. Here, we would expect to observe a progressive decrease in λ_1 if the rotation of the OH group and its conjugation with the b_1 orbital became increasingly inhibited by the ortho *t*-Bu groups. Since the observed trend shows an increase in λ_1 we conclude that the OH group can rotate freely even with *t*-Bu groups occupying both ortho positions and that *t*-Bu has a slightly greater inductive effect than Me. If the rotation of the OH group were inhibited, the oxygen n(p) orbital would not conjugate with the ring and a single CT absorbance would occur near 350 nm rather than at 450–550 nm as observed. Finally, the *K* values decrease from 0.90 L/mol to nil indicating that steric hindrance to intermolecular interaction increases progressively in the same series. Comparison of the characteristics of **35MP–T** and **35BP–T** supports the above conclusions.

Table 2. Shifts in Absorbance Maxima for TCNE Complexes of Methyl- and *tert*-Butylphenols as a Function of Methyl Position on Ring

			$\Delta\lambda_1$/R					$\Delta\lambda_2$/R		
donor	λ_1	$\Delta\lambda_1$	*o*	*m*	*p*	λ_2	$\Delta\lambda_2$	*o*	*m*	*p*
P	483					388				
2MP	*515*	*32*	*32*			*415*	*27*	*27*		
3MP	*510*	*27*		*27*		*420*	*32*		*32*	
4MP	535	52			52	394	4			4
23MP	*540*	*57*	*29*	*28*		*450*	*62*	*31*	*31*	
24MP	557	74	*27*		*47*	428	40	*35*		*5*
25MP	*540*	*57*	*29*	*28*		*440*	*52*	*26*	*26*	
26MP	*540*	*57*	*28*			*450*	*62*	*31*		
34MP	558	75		*27*	*48*	427	39		*34*	*5*
35MP	*535*	*52*		*26*		*450*	*62*		*31*	
mean			**29**	**27**	**49**			**30**	**31**	**5**
2BP	*526*	*43*	*43*			*428*	*40*	*40*		
3BP										
4BP	532	49			49	400	12			12
24BP	585	102	*48*		*54*	443	50	*40*		*10*
26BP	564	81	42			447	84	42		
mean			**44**		**51**			**40**		**11**

iii. Summary. Observations on the **T** complexes of the methylbenzenes[12] indicate that methyl groups which are ortho or meta to a reference methyl on the benzene ring elevate the values of both λ_1 and λ_2 by 25–30 nm per methyl whereas methyl groups which are para to a reference methyl elevate the value of λ_1 by about 40 nm but have practically no effect on λ_2.

The same patterns are observed for the wavelength shifts for **T** complexes of the methylphenols relative to **P–T**; these are summarized in Table 2. Values of λ_1 and λ_2 appear in columns 2 and 7. The gross wavelength shift values, $\Delta\lambda_1$ and $\Delta\lambda_2$ in columns 3 and 8, are obtained by subtracting the λ_1 and λ_2 of each of the methylphenols from the corresponding values for **P–T**. The portion of the shift value, $\Delta\lambda_1$/Me or $\Delta\lambda_2$/Me, which is attributable to the inductive effect of each of the *o*-, *m*-, or *p*-methyls is given in columns 4–6 and 9–11. Estimated values are italicized; mean values are given in the bottom row in bold type. The results indicate that (1) methyl groups which are ortho or meta to the OH group on the benzene ring elevate the values of both λ_1 and λ_2 by 25–35 nm per methyl whereas (2) methyl groups which are para to a reference methyl elevate the value of λ_1 and λ_2 by about 45–50 and 5 nm. The wavelength for a methylphenol–**T** complex can be estimated using the empirical formulas

$$\lambda_1 = 483 + 28(n_o + n_m) + 49n_p \qquad (2)$$

$$\lambda_2 = 388 + 30(n_o + n_m) + 5n_p \qquad (3)$$

---

[17] Maier, J. P.; Turner, D. W. *J. Chem. Soc., Faraday Trans. 2* **1973**, *69*, 521–531.

which are based on the analysis of wavelengths of nine methylphenol–T complexes (Table 2). Here n_o, n_m, and n_p are the number of *o*-, *m*-, or *p*-methyls per molecule, and the coefficients are weighting factors for each methyl. The coefficients reflect the relative inductive effect of the methyl group with respect to its location on the ring. The fact that one parameter suffices for both *o*- and *m*-methyls indicates that rotation of the OH group is not hindered in these compounds. The data for the *tert*-butylphenol complexes suggest that the rotation of the OH group is not even hindered by *tert*-butyl groups in the ortho positions.

d. Trialkylphenols. Four of the six possible trimethylphenol–**T** systems are characterized in this study. The ϵ and K values fall within the range of 2300–3500 L/mol-cm and 1.8–2.3 L/mol. Again, it is convenient to divide the discussion of these systems into two parts: (i) systems which yield spectra with two distinct maxima, i.e, those in which the phenol contains a 4-Me group and (ii) systems which exhibit a composite band with only one maximum.

i. 246MP–T and 345MP–T. These complexes have nearly identical values of λ_1 (583, 574 nm) and λ_2 (467, 465 nm). The fact that λ_1 for **246MP–T** is not smaller than that for **345MP–T** is further evidence of the lack of appreciable steric hindrance to the rotation of the OH group into a coplanar conformation by the *o*-Me's on the ring. Calculation of λ_1 and λ_2 by eqs 2 and 3 yields values 588 and 453 nm in excellent agreement with experiment.

ii. 235MP–T and 236MP–T. The characteristics of these complexes are nearly identical in all respects. Their spectra each consist of a broad symmetrical band with λ_{max} 515 nm and $\Delta\nu_{1/2}$ 7000–7100 cm^{-1}. Calculation of λ_1 and λ_2 by eqs 2 and 3 yields values of 567 and 478 nm; the average of these values, 523 nm, is close to the observed λ_{max} indicating that the observed bands are composites of two overlapping CT bands of similar height. CT bands due to single transitions usually have $\Delta\nu_{1/2}$ values of 5000–6000 cm^{-1}.

e. Hydroxybenzenes. The low solubilities of most of the di- and trihydroxybenzenes in DCM restrict the range of studies of their complexes with **T**. The insolubility of **4HOP** precluded the investigation of its interactions with **T** in DCM.

i. Dihydroxybenzenes. The spectrum of **2HOP–T** consists of two distinct bands at λ_1 540 and λ_2 430 nm; these values indicate that the hydroxyl groups act in concert to elevate the energies of both a_2 and b_1 orbitals relative to **P–T** and that an *o*-OH is more effective in this regard than an *o*-Me. Presumably, both hydroxyls in **2HOP** are able to conjugate effectively with the ring orbitals without steric interference. The I_1 and I_2 values of 8.56 and 9.25 eV[18] for **2HOP**, however, yield calculated values of λ_1 467 and λ_2 386 nm for **2HOP–T**.

The spectrum of **3HOP–T**, consisting of a broad unsymmetrical band ($\Delta\nu_{1/2}$ 9100 cm^{-1}) with λ_{max} 505 nm, is undoubtedly a composite of two strongly overlapping CT bands. The I_1 and I_2 values of 8.63 and 9.15 eV[18] for **3HOP** yield calculated values of λ_1 456 and λ_2 396 nm for **3HOP–T** which are both lower than the observed value. The spectrum of **2M3HOP–T** consists of a narrower band ($\Delta\nu_{1/2}$ 6500 cm^{-1}) with λ_{max} 507 nm indicating that λ_2 has increased and λ_1 has not changed relative to **3HOP–T**.

Spange et al.[19] report values of λ_1 588 and λ_2 381 nm for **4HOP–T** in MeCN which indicate a strong additive conjugative effect of both OH groups on the b_2 orbital. The I_1 and I_2 values of 8.44 and 9.66 eV[18] yield calculated values of only 485 and 350 nm.

The striking discrepancies between the experimental and calculated values of λ_1 and λ_2 for **2-**, **3-**, and **4HOP–T** suggest that the OH groups in the dihydroxybenzenes are coplanar with the ring in the complexes but are not coplanar under conditions in which PE spectra are obtained.

ii. Trihydroxybenzenes. The spectrum of **23HOP–T** consists of a symmetrical band with λ_{max} 516 nm and $\Delta\nu_{1/2}$ 6500 cm^{-1}. The shift in λ_{max} relative to those of **3HOP–T** and **2M3HOP–T** (505 and 507 nm) indicates that the additional hydroxyl contributes to the enhancement of conjugation in the b_1 and a_2 orbitals. The similarity of the λ_{max} value of **23HOP–T** (516 nm) with that of **35HOP–T** in MeCN (514 nm) reported by Spange[19] indicates that there is no appreciable steric interaction between the three adjacent OH groups in **23HOP**.

f. Summary and Conclusions. (1) CT Bands. CT complexes of methyl and hydroxyl derivatives of **P** exhibit corresponding bands which are shifted depending on the location and character of the substituent group. Methyl groups which are ortho or meta to the reference hydroxyl interact inductively with both the b_1 and a_2 orbitals whereas a methyl para to the reference hydroxyl interacts only with the b_1 orbital. Hydroxyl groups in corresponding positions with reference to the hydroxyl interact conjugatively with the b_1 and a_2 orbitals.

(2) Association Constants and Molar Absorbances. Inspection of the trends in K values of 12 methylphenol–**T** complexes (Table 1) indicates that log K tends to increase with the number of methyl substituents per molecule, n. A plot of log K versus n yields the linear relationship

$$\log K = \log K_0 + Bn = -0.492 + 0.253n \qquad (4)$$

where K_0 is the association constant of **P–T**. The correlation coefficient, r, is 0.958.

A plot of log (ϵK) for the same complexes also yields a linear relationship with respect to n where r equals 0.989.

$$\log (\epsilon K) = \log (\epsilon K)_0 + B'n = 2.68 \pm 0.36n \qquad (5)$$

Here, $(\epsilon K)_0$ is the ϵK product for **P–T**. In principle, it should be possible to estimate values of ϵ and K for any methylphenol–**T** complex by combining eqs 4 and 5.

The preceding summary shows that both the CT energies and association constants for the methylphenol–**T** complexes are linearly related to the number of methyl substituents on the phenol ring. It follows that the thermodynamic stability of this family of complexes arises from CT interactions between the donor and acceptor molecules.

(3) Inductive Effects. Replacement of a methyl on a phenol ring by a series of progressively bulky alkyls produces a slight increase in λ_{max} values of alkylphenol–**T** complexes indicating that the inductive effect increases in the order Me < Et < *i*-Pr < *t*-Bu.

(4) Steric Effects. K values of a series of alkylphenol–**T** complexes decrease in the order Me > Et > *i*-Pr > *t*-Bu indicating that bulky substituents interfere with intermolecular contact between the donor and acceptor orbitals.

---

[18] Palmer, M. H.; Moyes, W.; Speirs, M.; Ridyard, J. N. A. *J. Mol. Struct.* **1979**, *52*, 293–307.

[19] Spange, S.; Maenz, K.; Stadermann, D. *Liebigs Ann. Chem.* **1992**, 1033–1037.

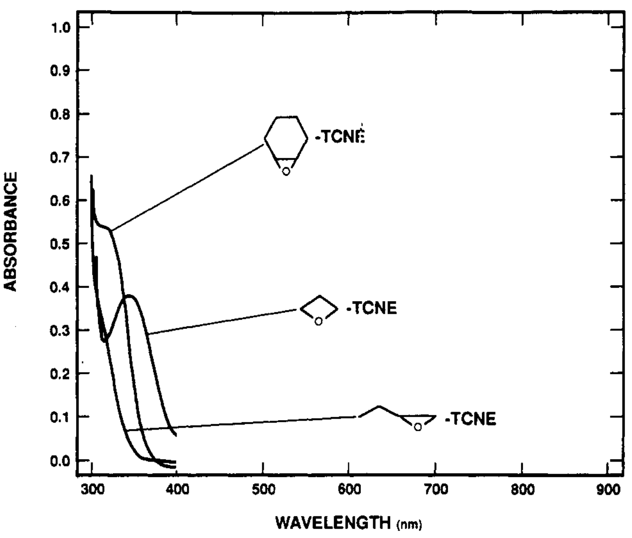

Figure 4. Spectra of oxetane–, ethyloxirane–, and cyclohexene oxide–T.

Replacement of *o*-Me by *t*-Bu groups in **26MP–T** and **246M-T**, however, does not diminish λ_{CT} values, indicating that rotation of the OH group is not hindered by intramolecular interference with ortho *t*-Bu groups.

3. Alkyl Ethers and Peroxides. The HOMO of an alkyl ether is the nonbonded $n(b_1)$ orbital of the oxygen atom which has a symmetry suitable for overlap with the LUMO of **T**. Evidence presented below indicates that CT bands in **T** complexes of alkyl ethers arise from a $\pi^* \leftarrow n(b_1)$ transition.

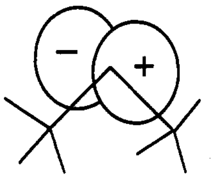

$n(b_1)$ Orbital of Methyl Ether

a. Acyclic Ethers. The only CT complex of **T** with an open-chain alkyl ether described prior to this study is that of **EEO–T** in $CHCl_3$ with a reported λ_1 of 335 nm.[1] We observed one band each for **EEO–T** and **IIO–T** with λ_1 347 nm. The spectra of the **BMO–T** and **BEO–T** systems exhibit higher λ_1 values of 355 and 360 nm reflecting the greater inductive effect of the *tert*-butyl group. Analysis of the spectral data for these systems yield Scott lines with a nearly zero slope indicating that the ethers form contact CT complexes with **T**.

The I_1 values of **EEO**, 9.73 eV,[20] and **BMO**, 9.44 eV,[21] correspond to calculated values of 344 and 368 nm for λ_1 values of **EEO–T** and **BMO–T** in excellent agreement with observation. The first ionization of **EEO** arises from the $n(b_1)$ orbital of the oxygen atom indicating that the CT band of the complex is due to a $\pi^* \leftarrow n(b_1)$ transition.

b. *tert*-Butyl Peroxide. The spectrum of the **BBOO–T–DCM** system appears as a shoulder on the **BBOO** cutoff at 375 nm. The deconvoluted band of **BBOO–T** has λ_{max} 385 nm with $\Delta\nu_{1/2}$ 9000 cm^{-1} indicating that it is a composite of two overlapping CT bands. Batich and Adam[22] report that the PE spectrum of **BBOO** has a single ionization band with I_1 8.78 eV which is consistent with a molecule in a *s*-*trans*-planar conformation. On this basis we would expect the spectrum of **BBOO–T** to appear as a relatively narrow band with λ_1 438 nm. The lack of agreement between the observed and predicted spectrum suggests that **BBOO** has a staggered conformation, $\angle$C-O-O-C $\approx$ 90°, in the complex. It is interesting to note that the PE spectrum of 3,3,6,6-tetramethyl-1,2-dioxane, which has a staggered conformation about the O–O bond, consists of two closely spaced ionization bands at about 9.55 eV. This pattern is consistent with the CT spectrum of **BBOO–T** and supports the assignment of a staggered conformation of **BBOO** in the complex.

c. Cyclic Ethers. In this section we examine characteristics of complexes of **T** with donors in which the oxygen is bound in triatomic (oxirane), tetratomic (oxetane), pentatomic (furan), and hexatomic (pyran) rings.

i. Oxiranes. The spectrum of the complex of **T** with **12BO** (ethyloxirane) consists of a steep shoulder with λ_{max} from 300 to 325 nm (Figure 4). McAlduff and Houk[23] report that I_1 of **12BO** is due to the loss of an electron from the $n(b_1)$ orbital of oxygen. The λ_1 calculated from I_1 (10.15 eV) at 315 nm is close to the estimated value for the complex indicating that the CT band clearly arises from a $\pi^* \leftarrow n(b_1)$ transition.

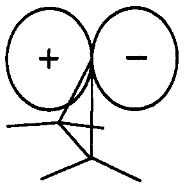

$n(b_1)$ Orbital of Oxirane

This interpretation is supported by evidence from the spectrum of the complex of **T** with **12CHO** (structurally similar to a *cis*-dialkyloxirane) which exhibits a distinct maximum at 315 nm on the shoulder of the **T** cutoff. Although its value has not been reported, I_1 for **12CHO** is expected to be about equal to that of *trans*-1,2-dimethyloxirane, I_1 9.98 eV.[23] The estimated value of λ_1 for **12CHO–T** at 320–325 nm is in good agreement with experiment.

ii. Oxetane. The spectrum of **OXT–T** consists of a band with λ_1 340 nm. Mollère and Houk[24] showed that the $n(b_1)$ orbital of oxetane should have a lower I_1 value than that of the highly-strained oxirane. Their expectation is borne out by the I_1 value of **OXT** at 9.63 eV which corresponds to a calculated value of 352 nm for **OXT–T**.

iii. Tetrahydrofuran and Tetrahydropyran. The λ_1 values of the complexes of the unstrained cyclic ethers **THF–T** and **THP–T** at 340 and 335 nm are essentially identical to that of **EEO–T** at 335 nm. The I_1 values of **THF** and **THP**, 9.57 eV[25] and 9.49 eV,[20] yield calculated λ_1 values of 357 and 364 nm for the **T** complexes.

d. Summary. (1) The alkyl ethers form contact CT complexes with **T** having a single absorbance band at 347 nm. This band is due to an electron arising from the $n(b_1)$ orbital of the oxygen atom. The dialkyl peroxide, di-*tert*-butyl peroxide, also forms a well characterized complex with **T**.

---

[20] Behan, J. M.; Dean, F. M.; Johnstone, R. A. W. *Tetrahedron* **1976**, *32*, 167–171.

[21] Turner, D. W. *Molecular Photoelectron Spectroscopy*; Wiley-Interscience: London, 1970; p 380.

[22] Batich, C.; Adam, W. *Tetrahedron Lett.* **1974**, 1467–1470.

[23] McAlduff, E. J.; Houk, K. N. *Can. J. Chem.* **1977**, *55*, 318–331.

[24] Mollère, P. D.; Houk, K. F. *J. Am. Chem. Soc.* **1977**, *99*, 3226–3233.

[25] Bain, A. D.; Bünzli, J. C.; Frost, D. C.; Weiler, L. *J. Am. Chem. Soc.* **1973**, *95*, 291–292.

(2) The cyclic alkyl ethers studied in this investigation form 1:1 complexes with **T**. The complexes of the highly strained oxiranes have λ_1 values of 300–315 nm indicating that the extreme strain in the oxirane ring stabilizes the n(b_1) orbital. The **T** complexes of the four-, five-, and six-membered ring ethers have λ_1 values which are similar to those of acyclic ethers.

4. Alkyl and Aryl Vinyl Ethers. a. Alkyl Vinyl Ethers. Williams et al.[26] observed that alkyl vinyl ethers form colored solutions on mixing with **T** and that their colors fade as the reactants form cyclobutane adducts. Ledwith and Woods[8] showed that these colors arise from CT transitions in $ROCH{=}CH_2$–**T** complexes and reported that λ_{CT} values increase in the order R = Me (401 nm) < Et (419 nm) < *i*-Pr (430 nm) < *t*-Bu (436 nm). They argued that the behavior of **MVO** is governed by a conjugative interaction between the n(b_1) orbital of the alkoxy group and the π orbital of the double bond that occurs only when the molecule is in a planar *cis*- or *trans*-conformation. They attributed the observed trend in λ_{CT} to strain effects of the branched alkyls which force the molecule into the *gauche*-conformation where conjugation is inhibited.

Friege and Klessinger[27] reported PE ionization bands for the alkyl vinyl ethers $ROCH_2{=}CH_2$ (R = Me, Et, *i*-Pr, *t*-Bu) at 9.14, 9.15, 8.84, and 8.77 eV. The calculated λ_{CT} values for the corresponding $ROCH{=}CH_2$–**T** complexes at 396, 401, 431, and 439 nm are in good agreement with the experimental values above. However, they attribute the PE bands to ionizations from conjugated orbitals of the type π[C═C]–n[O] (for the *s*-*cis*-conformer) and π-[C═C]–n[O]–π[CH_3] (for the *s*-*trans*-conformer). They postulate that the *s*-*cis*-conformation, with a lower degree of conjugation and a lower HOMO energy, is preferred by the unhindered methyl and ethyl vinyl ethers. Furthermore, the *s*-*trans*-conformation (rather than the *gauche*-conformation proposed by Ledwith and Woods) is preferred by the sterically hindered isopropyl and *tert*-butyl vinyl ethers. The fact that higher values of λ_{CT} are usually associated with greater conjugation in a series of related complexes supports the position of Friege and Klessinger.

The value of λ_{CT} exhibited by the complex of **T** with methyl 2-propenyl ether[8] is 452 nm; this corresponds to a $\Delta\lambda_{CT}$ shift of 51 nm relative to **MVO–T**. This shift is due solely to the inductive effect of the methyl adjacent to the double bond.[12] The complexes of the cyclic vinyl ethers 3,4-dihydro-2*H*-pyran (**34DHP**) and 2,3-dihyrofuran (**23DHF**) exhibit λ_{CT} values of 487 and 503 nm which correspond to $\Delta\lambda_{CT}$ shifts of 86 and 102 nm relative to λ_{CT} for **MVO–T**. The shift values for **34DHP–T** and **23DHF–T** are enhanced because the oxygens are locked into an orientation which optimizes π[C═C]–n[O] conjugation. The I_1 value of 8.68 eV for **34DHP** reported by Planckaert et al.[28] yields a calculated value of λ_{CT} 451 nm.

The complex of **T** with **25DHF**, in which the double bond and oxygen are unconjugated, exhibits a broad band ($\Delta\nu_{1/2}$ 6500 cm^{-1}) with λ_{CT} 389 nm. This values lies between the λ_{CT} values for cyclohexene–T (415 nm) and **THF–T** (340 nm) which indicates that the band is a composite of two overlapping bands arising from independent interactions of **T** with C═C and oxygen.

Finally, we attempted to determine *K* values for several of these complexes. Since the cycloaddition reactions were fairly rapid with some systems, valid absorbance data were obtained by measuring log *A* with respect to time and extrapolating log *A* to zero time. This procedure was effective for the **23DHF–T**; however, 1- and 2-butyl vinyl ether–T systems reacted so rapidly that erratic results were obtained. *K* values of 0.29, 0.23, and 0.41 L/mol are reported for **34DHP–T**, **23DHF–T**, and **25DHF–T**.

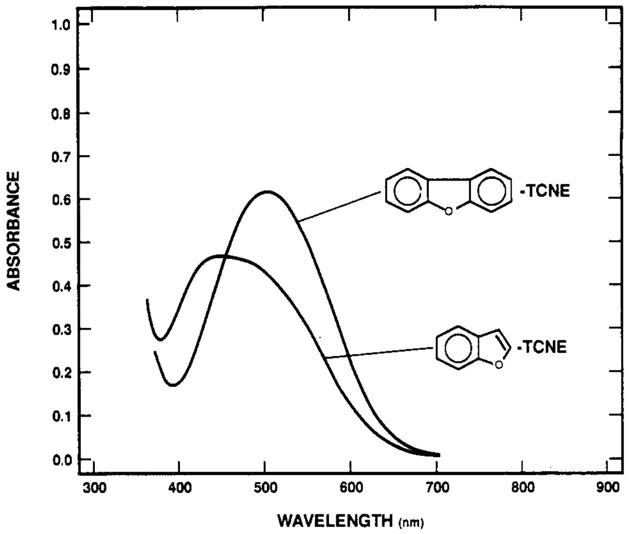

Figure 5. Spectra of benzofuran– and dibenzofuran–T.

b. Benzofuran. The spectrum of **BF–T** (Figure 5) consists of a broad (8000 cm^{-1}) unsymmetrical band (λ_{max} 460 nm) which is clearly a composite of two strongly overlapping bands with estimated values of λ_1 *500* and λ_2 *425* nm. The I_1 and I_2 values of **BF**[29] at 8.36 and 8.89 eV correspond to λ_1 498 and λ_2 425 nm. Buemi et al.[30] assign these ionizations to electrons from the 5a″ and 4a″ orbitals.

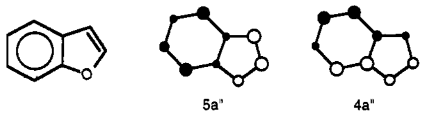

π Molecular Orbitals of Benzofuran

The 5a″ orbital is delocalized over both rings through π–π conjugation with the ethene moiety, and the 4a″ orbital is delocalized over both rings through n(b_1)–π conjugation with the oxygen.

c. Summary. Alkyl vinyl ethers form complexes with **T** which exhibit a single band with λ_{CT} 400–435 nm. The λ_{CT} value tends to increase with the bulk of the alkyl substituent, since the larger substituents are forced into the *s*-*trans*-conformation in which extensive π[C═C]–n[O]–π[CH_3] conjugation occurs. Cyclic vinyl ethers have higher λ_{CT} values because the double bond and oxygen are forced into conformations which optimize conjugation. The complex of **T** with **BF** exhibits two CT bands which arise from orbitals formed by the conjugation of the O–C═C fragment with the benzene ring.

5. Aryl Ethers. a. Diphenyl Ether. Various experimental[31–33] and theoretical[34,35] studies of **PPO**

---

(26) Williams, J. K.; Wiley, D. K.; McKusic, B. C. *J. Am. Chem. Soc.* **1962**, *84*, 2210–2215.

(27) Friege, H.; Klessinger, M. *J. Chem. Res., Synop.* **1977**, 208–209.

(28) Planckaert, A. A.; Doucet, J.; Sandorfy, C. *J. Chem. Phys.* **1974**, *60*, 4846–4853.

(29) Eland, J. H. D. *J. Mass Spectrom. and Ion Physics* **1969**, *2*, 471–484.

(30) Buemi, G.; Zuccarello, F.; Romeo, G. *J. Mol. Struct.* **1983**, *105*, 375–383.

(31) Le Fèvre, R. J. W.; Saxby, J. D. *J. Chem. Soc. B* **1966**, 1064–1066.

(32) Buchanan, G. W.; Montaudo, G.; Finocchiaro, P. *Can. J. Chem.* **1974**, *52*, 767–774.

(33) Llabrès, G.; Baiwir, M.; Christiaens, L.; Piette, J.-L. *Can. J. Chem.* **1979**, *57*, 2967–2970.

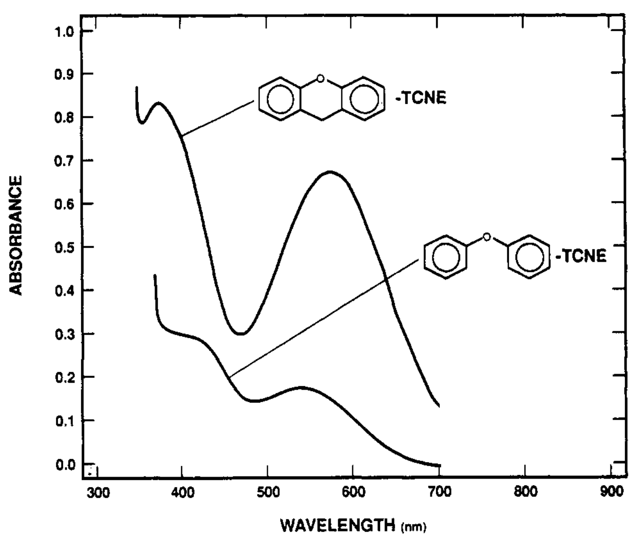

Figure 6. Spectra of diphenyl ether– and xanthene–T.

suggest that the twist angle with respect to the C–O–C plane is 30–50° and that there is significant n(b_1)–π conjugation in the molecule. This interpretation of the conformation of **PPO** is supported by the presence of two distinct bands λ_1 490 and λ_2 375 nm in the spectrum of **PPO–T** (Figure 6). The λ_2 band at 375 nm arises from an $\pi^* \leftarrow a_2$ transition. The fact that it is slightly lower in wavelength than the λ_{CT} band of benzene–T at 385 nm indicates that the oxygen inductively withdraws electronic charge from the phenyl ring. The I_2 value of **PPO**[27] at 9.10 eV corresponds to a λ_2 of 401 nm. The λ_1 band at 490 nm arises from the delocalized orbital resulting from n(b_1)–π conjugation. The I_2 value of **PPO** at 8.35 eV corresponds to λ_2 of 499 nm.

b. Dibenzofuran. The spectrum of **DBF–T** (Figure 5) contains a symmetrical band (6300 cm^{-1}) with λ_{CT} 500 nm and a broad shoulder at 310–390 nm. **DBF**[36] is planar with C_{2v} symmetry. The first cluster in its PE spectrum[37] resolves into two bands with maxima at 8.19 and 8.40 eV which are attributed to ionizations from the $4b_1$ and $3a_2$ orbitals. These ionizations correspond to overlapping CT bands at 527 and 485 nm consistent with the observed broad CT band centered at 500 nm. The broad shoulder in the **DBF–T** spectrum is due in part to three absorbance peaks in the UV spectrum of DBF at 323sh, 338, 356, and 375 nm and to a CT transition in this region. The PE spectrum of **DBF** has an ionization band at 9.35 eV corresponding to a CT band at 377 nm.

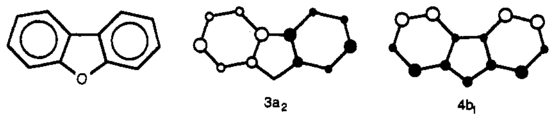

π Molecular Orbitals of Dibenzofuran

The Scott lines for **DBF–T** systems are always strongly curved when **DBF** is in excess, indicating that 2:1 complexes form readily in this system. Values of ϵ and K of 603 L/mol-cm and 1.36 L/mol are obtained by analysis of a system containing excess **T**.

c. Xanthene. The spectrum of **XAN–T** (Figure 3) consists of two bands λ_1 575 and λ_2 375 nm. Analysis of spectra of systems containing excess **XAN** always yields strongly curved lines indicating the presence of appreciable quantities of the **D$_2$T** species. Molecular polarizability studies[38] indicate that the dihedral angle between the phenyl rings in **XAN**, 160 ± 6°, is favorable for n(b_1)–π conjugation. The inductive effect of the *o,o'*-methylene group is expected to enhance the energy of the HOMO and to give rise to a λ_1 value greater than 500 nm. The second HOMO of **XAN** is not expected to participate in conjugation and should therefore give rise to a band $\lambda_2 <$ 385 nm. The values of λ_1 375 and λ_2 575 nm are consistent with these expectations.

d. Summary. Mixtures of **T** with excess **PPO**, **DBF**, and **XAN** yield strongly curved Scott lines indicating the presence of both **DT** and **D$_2$T** complexes. However, 1:1 species are readily characterized in systems containing excess **T**. Spectra of these complexes exhibit two bands each, λ_1 490–575 and λ_2 375 nm, which are attributed to $\pi^* \leftarrow \pi$ transitions. The λ_1 bands show evidence of n(b_1)–π conjugation, whereas the λ_2 bands are localized on the benzene rings and show evidence of electron withdrawal through the inductive effect of oxygen.

6. Furans. a. Furan. The spectrum of **F–T** exhibits a symmetrical band λ_1 449 nm and evidence for a second absorbance near 300 nm. This observation is consistent with PE studies of Klasinc et al.,[39] who attribute I_1 8.83 eV and I_2 10.39 eV of **F** to ionizations from the a_2 (node coincident with C_2 axis through oxygen) and b_1 (node through the 2- and 5-carbons) orbitals; these values correspond to λ_1 432 and λ_2 300 nm.

b. Alkylfurans. The spectrum of **2MF–T** exhibits bands λ_1 512 and λ_2 312 nm in expectation of a strong inductive effect for the 2-Me on the a_2 orbital and of a weak effect on the b_1 orbital. The spectrum of **25MF–T** exhibits bands λ_1 547 and λ_2 329 nm. The λ_1 shift of **25MF–T** relative to **F–T** (125 nm) is double the λ_1 shift observed for **2MF–T** (63 nm), indicating that the inductive effects of the 2- and 5-Me are additive. The corresponding λ_2 shifts are very small since the node of the b_1 orbital coincides with the 2- and 5-positions.

Aliosi et al.[4] report that **3MF–T** has λ_1 490 nm; this indicates that the inductive effect of a 2-Me on the a_2 orbital is somewhat more pronounced than that of a 3-Me. Aliosi reported that this same trend is observed in **2BF–T** with λ_1 530 nm and **3BF–T** with λ_2 490 nm. These experimental results are compatible with HMO calculations of Galasso et al.,[40] which indicate that the electron density of the HOMO is maximal at the 2- and 5-positions.

7. Alkyl Phenyl Ethers. a. Anisole. The spectrum of **A–T** exhibits two bands λ_1 511 and λ_2 389 nm. Bock et al.[41] observed ionization bands I_1 8.42 and I_2 9.23 eV which correspond to λ_{CT} values of 488 and 388 nm. They showed that the degeneracy of the e_{1g} orbitals of the phenyl ring is removed by n(b_1)–π(e_{1g}) conjugation between the

---

(34) Galasso, V.; De Alti, G.; Bigotto, A. *Tetrahedron* **1971**, *27*, 6151–6158.

(35) Rodin, O. G.; Traven, V. F.; Redchenko, V. V.; Eismont, M. Yu.; Stepanov, B. I. *J. Gen. Chem. USSR (Engl. Transl.)* **1983**, *53*, 2287–2292; *Zh. Obshch. Khim.* **1983**, *53*, 2537–2543.

(36) Dideberg, O.; Dupont, L.; André, J. M. *Acta Crystallogr.* **1972**, *B28*, 1002–1007.

(37) Rodin, O. G.; Redchenko, V. V.; Kostitsyn, A. B.; Traven, V. F. *J. Gen. Chem. USSR (Engl. Transl.)* **1988**, *58*, 1256–1261; *Zh. Obshch. Khim.* **1988**, *58*, 1409–1415.

(38) Aroney, M. J.; Hoskins, G. M.; Le Fèvre, R. J. W. *J. Chem. Soc. B* **1969**, 980–982.

(39) Klasinc, L.; Sablijic, A.; Kluge G.; Rieger, J.; Scholtz, M. *J. Chem. Soc., Perkin Trans. 2* **1982**, 539–543.

(40) Galasso, V.; Klasinc, L.; Sabljic, A.; Trinajstic, N.; Pappalardo, G. C.; Steglich, W. *J. Chem. Soc., Perkin Trans. 2* **1981**, 127–131.

(41) Bock, H.; Wagner, G.; Kroner, J. *Tetrahedron Lett.* **1971**, 3713–3719.

nonbonded electron pairs of the oxygen and the symmetric e_{1g} orbital of the phenyl, giving rise to the conjugated b_1 orbital and the nonconjugated a_2 orbital.

In this connection, we note that λ_1 for **A–T** at 511 nm is 28 nm higher than λ_1 for **P–T**, revealing that the inductive effect of the methyl in **A** is added to the conjugative effect of the oxygen on the b_1 orbital. On the other hand, the λ_2 values of **A–T** and **P–T** are nearly identical, indicating that the inductive effect of the methyl is not transmitted into the a_2 orbital. We infer that λ_1 and λ_2 originate from $\pi^* \leftarrow b_1$ and $\pi^* \leftarrow a_2$ transitions. Analysis of **P–T** spectra yield ϵ 1360 L/mol-cm and K 0.80 L/mol.

b. Alkoxybenzenes. The spectra of the ROPh–T complexes[8] (R = Me, Et, *i*-Pr, 2-Bu) each exhibit two maxima; **BPO–T** (R = *t*-Bu) has a single broad band which resolves into bands at *390* and *462* nm. The λ_2 values (385–390 nm) of these complexes are in good agreement with values expected from $\pi^* \leftarrow a_2$ transitions.

The λ_1 values, however, increase in the sequence **BPO–T** (*462* nm) < **A–T** (505 nm) < **EPO–T** (513 nm) < **IPO–T** = **2MBPO–T** (522 nm). It is well known that the electron-donating ability of alkyl groups increases in the order Me > Et > *i*-Pr > *t*-Bu.[42] If we assume that λ_1 values for ROHP–T complexes parallel the trend in inductive effects then λ_1 for **BPO–T** is clearly out of line. The anomaly is explained by Friege and Klessinger[43] who report I_1 values of 8.45, 8.36, 8.42, and 8.77 eV for **A**, **EPO**, **IPO**, and **BPO** which correspond to λ_1 values of 484, 498, 488, and 453 nm for the matching **T** complexes. They deduced that conjugation between the p orbital of the oxygen and the e_{1g} orbital of the phenyl group is optimum when the α-carbon is coplanar with the phenyl ring and that this conformation occurs only when the movement of the alkoxy group is unhindered. Alkoxybenzenes with bulky substituents such as *t*-Bu exhibit anomalously high I_1 values, indicating that the oxygen p orbitals in these compounds are tilted at an angle to the ring which is unfavorable to conjugation. Consequently, λ_1 for **BPO–T** should be relatively low as observed.

The ϵ_1 (1250–2220 L/mol-cm) and K (0.24–0.43 L/mol) values reported for the ROPh–T complexes are relatively uniform. This is surprising in view of the fact that K values of related hydrocarbon–T complexes have been shown to decrease with increasing bulk of the substituent[12].

8. Alkyl Aryl Ethers. In the discussion on hydroxy- and alkoxybenzenes the substituent effect of the OR group was attributed to the strong electron-donating π-conjugative interaction which occurs when OR is coplanar with the ring. However, a weaker electron-withdrawing effect occurs through the σ-electron system from the highly electronegative oxygen regardless of the orientation of the OR group. In molecules where OR can assume a coplanar conformation the conjugative effect is dominant and inductive effect is overwhelmed. However, in molecules where the OR group is forced into an out-of-plane conformation by steric hindrance the inductive effect can be isolated and observed. Several examples of this sort are presented in sections 8 and 9.

a. Methylanisoles. The K values of the methylanisole–T complexes are somewhat higher (0.98–1.51 L/mol) than **A–T** (0.8 L/mol). The spectra of complexes of **T** with **2MA** and structurally related 2,3-dihydrobenzofuran (**23HBF**) exhibit two bands λ_1 (547 and 567 nm) and λ_2 (422 and 405 nm). The high λ_1 value for **23HBF–T** is due to the rigidity of the 5-membered ring which holds the oxygen atom in the conformation required for optimum conjugation. The λ_1 and λ_2 values for these complexes as well as **3MA–T** (532 and 425 nm) reflect the inductive effect of the 2- and 3-methyl substituents on the b_1 and a_2 orbitals of the phenoxy ring. The I_1 and I_2 values of 8.24 and 8.93 eV for **2MA**,[16] 8.22 and 9.09 eV for **23HBF**,[20] and 8.28 and 8.93 eV for **3MA**[16] correspond to λ_1 and λ_2 values of 518 and 420 nm for **2MA–T**, 521 and 402 nm for **23HBF–T**, and 511 and 420 nm for **3MA–T**.

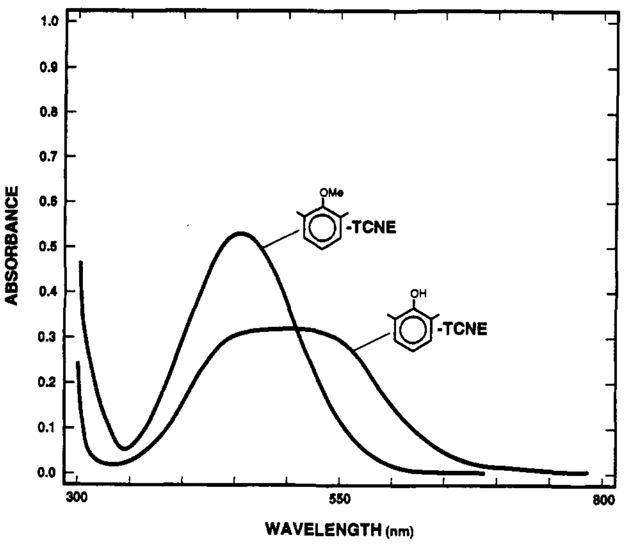

Figure 7. Spectra of 2,6-dimethylanisole– and 2,6-dimethylphenol–T.

A comparison of λ_1 563 nm and λ_2 395 nm values of **4MA–T** with those of **A–T** indicates that the 4-methyl substituent interacts strongly with the b_1 orbital but has little effect on the a_2 orbital. The I_1 8.18 and I_2 9.11 eV PE bands of **4MA** correspond to λ_1 529 and λ_2 400 nm for **4MA–T**.

b. Dimethylanisoles. All six possible dimethylanisole–T complexes were characterized. Values of K for the complexes fall in the range 0.55–2.26 L/mol. The donors are divided into two groups: (i) those which contain a 4-Me group and (ii) those which do not.

i. 24MA–T and 34MA–T. The spectra of these complexes are nearly identical, with **24MA–T** having λ_1 592 and λ_2 431 nm and **34MA–T** having λ_1 586 and λ_2 429 nm with a deep minimum between the peaks. The PE ionizations of **24MA** at 7.95 and 8.75 eV[20] yield calculated values of 574 and 442 nm. The similarity between the spectra indicates that a single *o*-Me does not diminish conjugation through steric interference with the rotation of the OMe group. The large difference between λ_1 and λ_2 values (161 and 157 nm) is attributed to the ability of the 4-Me group to supplement the strong inductive effect of the OH group on the b_1 orbital without affecting the a_2 orbital.

ii. 23MA–T, 25MA–T, 26MA–T, and 35MA–T. The λ_1 and λ_2 bands for these complexes overlap very strongly; three of the spectra exhibit shallow minima between the peaks, and only **26MA–T** (Figure 7) appears as single broad symmetrical band. Both λ_1 and λ_2 increase relative to the corresponding **A–T** bands due to the additive inductive effect of the two methyls on the b_1 and a_2 orbitals. The fact that λ_{max} 458 nm for **26MA–T** is lower than λ_2 470 nm for **35MA–T** indicates that the two *o*-Me's hinder the rotation of the OMe group sufficiently to inhibit n(p)–

---

[42] Hine, J. *Structural Effects on Equilibrium in Organic Chemistry*; Wiley-Interscience: New York, 1975; p 98.

[43] Friege, H.; Klessinger, M. *Chem. Ber.* **1979**, *112*, 1614–1625.

Table 3. Shifts in Absorbance Maxima for TCNE Complexes of Methylanisoles as a Function of Methyl Position on Ring

			$\Delta\lambda_1$/Me					$\Delta\lambda_2$/Me		
donor	λ_1	$\Delta\lambda_1$	*o*	*m*	*p*	λ_2	$\Delta\lambda_2$	*o*	*m*	*p*
A	511					389				
2MA	547	38	38			422	33	33		
3MA	532	21		21		425	36		36	
4MA	563	52			52	396	7			7
23MA	*560*	*49*	*32*	*17*		*465*	*76*	*37*	*39*	
24MA	594	83	*35*		*48*	431	42	*35*		*7*
25MA	574	63	*40*	*23*		454	65	*32*	*33*	
26MA[a]	*475*	*36*	*18*			*445*	*56*	*28*		
34MA	586	75		*22*	*53*	429	40		*34*	*6*
35MA	*545*	*34*		*17*		*465*	*76*		*38*	
mean			**36**	**20**	**51**			**34**	**36**	**7**

[a] **26MA** is excluded from the calculation of mean values because of steric effects.

$\pi(b_1)$ conjugation and to verify the presence of a weak electron-withdrawing inductive effect in these molecules.

It is interesting to compare the spectrum of **26MP–T**, which exhibits two bands (Figure 7), with that of **26MA–T**. In the latter case, rotation of the OMe is restricted by the *o*-Me's and conjugation is inhibited; in the first case the absence of steric interaction between the OH and the *o*-Me's in the donor molecule allows $n(p)-\pi(b_1)$ conjugation and the splitting of the a_2 and b_1 orbitals.

iii. Summary. The patterns observed for the wavelength shifts for **T** complexes of the methylanisoles relative to **A–T** are summarized in Table 3. Values of λ_1 and λ_2 appear in columns 2 and 7. The gross wavelength shift values, $\Delta\lambda_1$ and $\Delta\lambda_2$ in columns 3 and 8, are obtained by subtracting the λ_1 and λ_2 of each of the methylanisoles from the corresponding values for **A–T**.

The portion of the shift value, $\Delta\lambda_1$/Me or $\Delta\lambda_2$/Me, which is attributable to the conjugative/inductive effect of each of the *o*-, *m*-, or *p*-methyls is given in columns 4–6 and 9–11. Estimated values are italicized; mean values, given in the bottom row in bold face, do not include data for **26MA–T**. The results indicate that methyl groups which are meta to the OMe group on the benzene ring elevate the values of λ_1 by 15–25 nm and λ_2 by 30–40 nm per methyl whereas methyl groups which are para to a reference methyl elevate the value of λ_1 by 50 nm and λ_2 by 7 nm. If only one *o*-Me is present both λ_1 and λ_2 are elevated by 30–40 nm, whereas two *o*-Me's prevent the OMe group from attaining coplanarity with the ring and inhibit conjugation sufficiently to halve the normal λ_1 increment. The wavelength for a methylanisole–**T** complex can be estimated using the empirical formulas

$$\lambda_1 = 511 + 36n_o + 20n_m + 51n_p \text{ (for } n_o = 0,1) \qquad (6)$$

or

$$\lambda_1 = 511 + 18n_o + 20n_m + 51n_p \text{ (for } n_o = 2) \qquad (6')$$

$$\lambda_2 = 389 + 34n_o + 36n_m + 7n_p \text{ (for } n_o = 0,1) \qquad (7)$$

or

$$\lambda_2 = 389 + 28n_o + 36n_m + 7n_p \text{ (for } n_o = 2) \qquad (7')$$

which are derived from wavelength data for nine methylanisole–**T** complexes (Table 3). Here, n_o, n_m, and n_p are the number of *o*-, *m*-, or *p*-methyls per molecule. Note: If $n_o = 2$ the first weighting parameter in eq 6 must be changed from 36 to 18 and the corresponding parameter in eq 7 must be changed from 34 to 28. The weighting parameters reflect the relative inductive effect of each methyl group with respect to its location on the ring. The fact that two numerical variables are required for the *o*-Me's indicates that rotation of the OMe group is hindered by two *o*-Me's in these compounds.

c. Phenylanisoles. The spectrum of **4PA–T** exhibits bands λ_1 600 and λ_2 375 nm. The magnitude of λ_1 indicates that the phenyl group in **4PA** rotates freely with respect to the anisolyl group and that the two groups interact strongly through $\pi(b_1)-\pi(b_1)$ conjugation. The high value of λ_1 for **4PA–T** compared to **4MA–T** (563 nm) indicates that the conjugative effect of the phenyl is much more potent than the inductive effect of the methyl. The spectrum of **2PA–T** exhibits bands λ_1 550 and λ_2 415 nm which are nearly identical to those of **2MA–T**; this indicates that the substituent phenyl in **2PA** is unable to achieve coplanarity with the anisolyl group and that conjugation is inhibited because of steric interference between the phenyl and methoxy groups.

9. Polymethoxyarenes. When considering the overall effect of inductive and conjugative interactions on the orbital energies of the methoxybenzenes it is convenient to denote the reference substituent as the OMe group on the 1-carbon at the node of the $\pi(b_1)$ orbital. Then the $n(b_1)$ orbital of a *m*-OMe group interacts conjugatively and inductively with both the $\pi(b_1)$ and $\pi(a_2)$ orbitals and a *p*-OMe interacts exclusively with the $\pi(b_1)$ orbital. MO calculations show that an *o*-OMe group coplanar with the ring conjugates strongly with the $\pi(a_2)$ but only weakly with the $\pi(b_1)$ orbital. In addition, we note that an OMe group situated between two other *o*-OMe's has such severely hindered rotation that it is forced into an orientation perpendicular with the benzene ring. Such an OMe will be limited to a nearly unmixed inductive interaction with the ring.

a. Dimethoxybenzenes. The complex **2MOA–T** exhibits two bands λ_1 592 nm and λ_2 429. Anderson et al.[44] reported I_1 and I_2 values for **2MOA** of 8.17 and 8.94 eV which they found to be consistent with a model (based on STO-3G calculations) in which (a) the 1-OMe group lies in the plane of the ring with the Me rotated away from the 2-OMe group and (b) the 2-OMe is perpendicular to the plane of the ring and consequently not conjugated to the $\pi(b_1)$ orbital. These I_D values correspond to calculated values of λ_1 and λ_2 for **2MOA–T** of 530 and 419 nm. STO-3G calculations for a model in which both OMe's are coplanar yielded I_1 7.85 and I_2 8.80 eV. These calculated values correspond to λ_1 598 and λ_2 435 nm which are in excellent agreement with our observed values. This suggests that both OMe groups in **2MOA** are coplanar under the conditions in which it forms complexes with **T**.

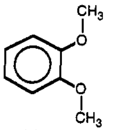

(a)

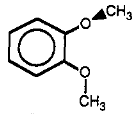

(b)

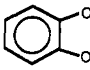

The spectra of the complex of **T** with 1,4-benzodioxane, **BDN**, exhibits λ_1 556 and λ_2 444 nm (Figure 8). **BDN** is structurally similar to **2MOA** except that the oxygens are bridged by a $-CH_2CH_2-$ group and are locked into a configuration in which neither oxygen is in the optimum

---

(44) Anderson, G. M.; Kollman, P. A.; Domelsmith, L. N.; Houk, K. N. *J. Am. Chem. Soc.* **1979**, *101*, 2344–2352.

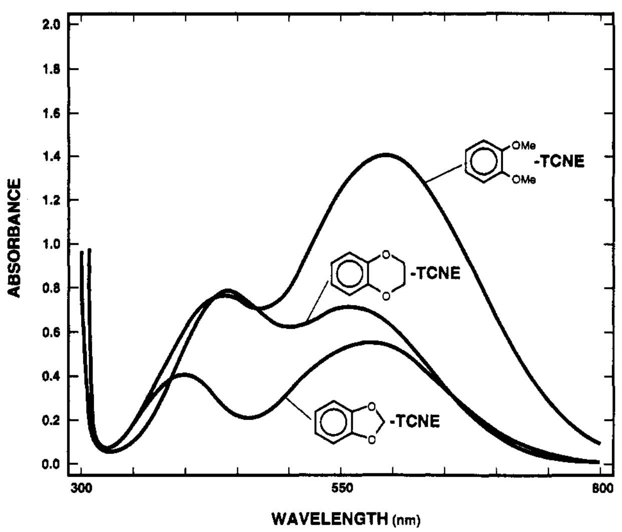

Figure 8. Spectra of 1,2-dimethoxybenzene–, 1,4-benzodioxane–, and 1,3-benzodioxole–**T**.

conformation for conjugation. The relatively low value of λ_1 is consistent with the above interpretation of the spectrum of **2-MOA–T**.

Zweig et al.[45] reported λ_1 575 nm for the **T** complex of 1,3-benzodioxole, **BDL**. This donor is structurally similar to **2MOA** except that the two Me groups are replaced by a $-CH_2-$ bridge which locks the two oxygens into the configuration of optimum conjugation. The high value of λ_1 indicates that both oxygens are conjugated with the ring. The close agreement in λ_1 values for the **T** complexes of **2MOA** and **BDL** suggests that both OMe groups in **2MOA** conjugate strongly with the ring and that they are coplanar with the benzene ring.

The complexes **3MOA**– and **4MOA–T** each exhibit two bands λ_1 and λ_2 of *559* and *441* nm and 637 and 380 nm. The I_1 and I_2 values of **3MOA** at 8.14 and 8.94 eV and for **4MOA** at 7.90 and 9.16 eV are both consistent with planar models.[44] This indicates that conjugation is optimal in **3MOA** and **4MOA** as expected from the absence of steric barriers to the achievement of coplanarity. The difference, $\lambda_1 - \lambda_2$, for **4MOA–T** (252 nm) is about double the corresponding difference for **A–T** (122 nm), indicating that the conjugative effect of the *p*-OMe's is additive and that both of them conjugate strongly with the b_1 orbital. The calculated values of λ_1 and λ_2 for **3MOA–T** are 536 and 446 nm and for **4MOA–T** are 585 and 386 nm.

The *K* values of **2MOA–T**, **3MOA–T**, and **4MOA–T** at 1.12, 0.68, and 0.68 L/mol are comparable in magnitude. This fact indicates that **2MOA** is planar under the conditions of complex formation, since out-of-plane OMe groups would tend to hinder donor–acceptor interaction and cause a decrease in its relative *K* value.

b. Trimethoxybenzenes. The spectrum of **23MOA–T** consists of a single broad band ($\Delta\nu_{1/2}$ 6400 cm^{-1}) with λ_{max} 515 nm. The breadth of the band and the relatively low value of λ_{max} suggest that λ_1 and λ_2 bands overlap strongly and that the b_1 and a_2 orbital energies are nearly degenerate. A survey of crystal structures of *o*-trimethoxybenzene and related compounds[44] reveals that in most cases the outer methoxys are nearly coplanar, implying net conjugation with both b_1 and a_2 orbitals, whereas the inner methoxy is nearly perpendicular. It is interesting to note that λ_{max} values for both **3MOA–T** at 546 nm and **35MOA–T** at 551 nm are larger than that of **23MOA–T** at 515 nm implying that an OMe which is perpendicular to the plane of the ring exerts a net electron-withdrawing effect due to induction.

Zweig et al.[45] reported λ_{max} 530 nm for the **T** complex of the structurally related donor 1-methoxy-2,3-(methylenedioxy)benzene. In this case the 2- and 3-oxygens are joined by a $-CH_2-$ bridge which maintains both oxygens in orientations favorable for conjugation. The larger value of λ_{max} relative to **23MOA** indicates that additional conjugation occurs.

The spectrum of **35MOA–T** consists of a single band with λ_{max} 551 nm. Here, the rotation of all three OMe groups is unhindered and the net conjugation with both orbitals is optimal and equal. Consequently the b_1 and a_2 orbital energies in **35MOA** are degenerate and λ_1 and λ_2 are equal.

The spectrum of **24MOA–T** consists of two bands with λ_1 690 and λ_2 449 nm. The donor molecule has OMe groups both ortho and para to the 1-OMe group. Here we expect the λ_2 value to be about equal to that for **2MOA–T** (433 nm) and the λ_1 value to be somewhat higher that of **4MOA–T** (637 nm). Both of these expectations are fulfilled. The *K* values of the trimethoxybenzene–T complexes are about double those of the corresponding dimethoxybenzene complexes.

c. Tetramethoxybenzenes. The spectrum of **234MOA–T** consists of a broad band which is resolved into overlapping bands λ_1 *560* and λ_2 *480* nm. The relatively low value of λ_1 may be attributed to the restricted rotation of the 2- and 3-OMe groups which diminishes the net conjugation with the b_1 orbital. However, the λ_2 value is exceptionally high.

The spectrum of **235MOA–T** consists of a single band with λ_{max} 606 nm. Assuming that the 2- and 5-OMe groups are centered on the antinodes of the b_1 orbital and that the 5-OMe group has unrestricted rotation, we expect λ_{max} to have a value about 120 nm higher than the corresponding value for **23MOA–T** (λ_{max} 515 nm). The actual difference of 90 nm is in reasonable agreement with expectation. The high *K* value for **235MOA–T** at 3.79 L/mol is double that of the dimethoxybenzene–T complexes indicating that *K* values tend to rise with increasing methoxy substitution as long as contact between the donor molecule and **T** is not sterically inhibited.

The spectrum of **245MOA–T** has two widely separated bands λ_1 800 and λ_2 440 nm. In this case the donor has no hindered OMe groups; consequently all four of them conjugate strongly with the a_2 orbital and more weakly with the b_1 orbital.

d. Penta- and Hexamethoxybenzene. The spectra of **PMOB–T** and **HMOB–T** each consist of a single band with λ_{max} values of 610 and 512 nm indicative of the near degeneracy of the a_2 and b_1 orbitals. The low λ_{max} value of **HMOB–T** is due to the fact that all six of the OMe groups are rotationally hindered and that the molecule has a low degree of conjugation. The pale purple color reported for the complex[6] suggests that the upturned OMe groups strongly hinder the interaction of the donor molecules with **T**. It is noteworthy that the **T** complex of the highly symmetrical **35MOA**, with three unrestricted OMe groups has a higher λ_{max} 552 nm, than the complex of **HMOB** with six restricted OMe groups.

e. Summary. The spectra of the polymethoxybenzene–T complexes generally consist of two bands or one broad band which can be resolved into overlapping bands.

---

[45] Zweig, A.; Lehnsen, J. E.; Murray, M. A. *J. Am. Chem. Soc.* **1963**, *85*, 3933–3936.

The values of λ_1 and λ_2 are dependent upon the conjugative and inductive interactions of the methoxy groups; consequently, the magnitude of these values serves as a measure of the influence of these interactions.

Finally, all OMe groups which are coplanar with the ring exert a net electron-enhancing effect on the π orbitals through conjugation, whereas those which are perpendicular to ring exert a net electron-withdrawing effect on the ring through induction.

Conclusions

1. Complexes of T with alcohols and ethers exhibit one CT band with λ_1 values of 300–360 nm. Complexes of acyclic donors form contact CT complexes with K values less than 0.1 L/mol, whereas complexes of cyclic ethers have K values of 0.2–1.3 L/mol. The favorable orientation of the donor orbitals in the cyclic ethers accounts for the higher K values of their complexes. The CT bands in each case arise from a $\pi^* \leftarrow n$ transition. Differences in the values of K and λ_{CT} for these complexes arise from the inductive and steric effects of the substituent alkyl groups.

2. Complexes of T with aromatic oxygen compounds exhibit two bands, λ_1 at 480–800 nm and λ_2 at 375–480 nm, which arise from the transfer of electrons in molecular orbitals formed by the conjugation of the oxygen with an attached aryl group or with an α-double bond in a cyclic structure. K values range from 0.1 to 3.8 L/mol. Differences in the values of K and λ_{CT} for these complexes arise from the conjugative, inductive, and steric effects of the substituent alkyl and alkoxy groups. The orientations of orbitals in cyclic compounds are strongly influenced by structural factors.

Acknowledgment. We are grateful for financial support from the Faculty Research Grant Fund and the Office of the Vice-President for Academic Affairs of Northern Michigan University. We thank Prof. Rolf Gleiter of the Organisch-Chemisches Institut of Heidelberg University for his hospitality during the preparation of this paper and for his generous assistance in obtaining PE spectra of some of the compounds used in this study. We thank Dr. Peter Bischof for valuable discussions regarding the interpretation of PE spectra and related MO diagrams.